

Influence of longitudinal chromatism on on-axis vacuum acceleration by intense radially polarized laser beams

Spencer W. Jolly*

LIDYL, CEA, CNRS, Université Paris-Saclay, CEA Saclay, 91 191 Gif-sur-Yvette, France

(Dated: December 15, 2024)

We report with single particle simulations that longitudinal chromatism, a commonly occurring spatio-temporal coupling in ultrashort laser pulses, can have a significant influence in the on-axis longitudinal acceleration of electrons via high-power, tightly-focused radially polarized laser beams. This effect can be advantageous, and even more-so when combined with small values of temporal chirp. However, the effect can also be highly destructive when the magnitude and sign of the longitudinal chromatism is not ideal, even at very small magnitudes. This motivates the characterization and understanding of the driving laser pulses, and further study of the influence of similar low-order spatial-temporal couplings on such acceleration.

The acceleration of electrons to relativistic energies in vacuum is possible with a tightly focused, high power radially polarized laser beam (RPLB). The solution of the wave equation in focus produces a purely longitudinal field on axis, with a radial field towards the axis at points slightly off-axis [1]. This provides the motivation for using these beams to accelerate particles, either from rest or from modest energies, to relativistic energies [2, 3]. We simulate the effects of spatio-temporal couplings (specifically longitudinal chromatism, or chromatic focusing) on such acceleration in two different scenarios, limited to particles on-axis. Since longitudinal chromatism affects the field mainly longitudinally, the effects on the acceleration enabled by the purely longitudinal fields of the focused RPLB could be severe.

The most general case of vacuum laser acceleration by an RPLB is that where a test particle begins from rest (or with a moderate initial energy) and an RPLB focuses and overtakes the particle. The longitudinal field in the focal region, when the laser power is large enough, imparts a net kinetic energy on the particle after overtaking. Detailed studies have been done showing especially that with optimization of both the initial position of the test particle and the carrier-offset phase (CEP), the kinetic energy of the particle is always higher with decreasing duration and/or decreasing focused spot size [4]. These studies included particles beginning at rest and a large range of laser powers showing the suitability of the mechanism. Studies were also done including nonparaxial terms [5], off-axis fields [6] and even more complex interactions [7–9] showing that low energy-spread and collimation are indeed possible in a bunch of electrons with finite charge and size. Experimental results of this nature have been achieved in a low density neutral gas achieving 23 keV energies [10], and in a true vacuum, accelerating some electrons in a bunch from 40 keV up to a maximum of 52 keV [11].

Because this mechanism requires essentially for the particle to gain enough energy in a single half-cycle so as to not be fully decelerated in a subsequent cycle, there is a threshold power below which the particle will gain

negligible energy. This has been shown to be related to the normalized beam intensity, and scales with the beam waist (w_0) as w_0^4 [12]. Above this threshold the particle gains significant energy, which is increasing with laser power. Well above the threshold the main limitation is that the accelerated particle inevitably slips out of the position of highest accelerating field since it is always travelling with a subluminal velocity. The maximum electron energy from a transform limited pulse has been shown to scale with the beam power (P) as \sqrt{P} , with higher intensity pulses approaching this limit [4].

The second scenario we approach is a restriction of the general case relating to electron acceleration from the interaction of an intense laser with a plasma mirror. In this complex nonlinear interaction the intense linearly polarized laser creates an overdense plasma at the surface, which then oscillates relativistically [13]. This mechanism can produce electrons ejected from the oscillating surface, which were observed to be accelerated in vacuum ponderomotively by the transverse field of the reflecting linearly polarized laser field [14]. There have been numerical studies showing that it is possible to have on-axis acceleration to high energies with the interaction of a radially polarized beam with such a plasma mirror [15]. This latter phenomenon is the result the same basic physics as the more general case of RPLB acceleration, with the most important contrast being that in this case the electrons begin with some energy (~ 0.2 MeV) and they are born from the plasma mirror oscillation within the focal volume at a set phase close to the optimum for acceleration [16]. Practically this means that the initial energy and position of the particle are fixed, where in the general scenario only the electrons with a certain initial position are accelerated well.

Beyond the use of a single Fourier-limited beam interacting with a single particle or bunch of particles, it may be possible to optimize the interaction with more complex or structured pulses, which we demonstrate in this work. A study was done in the general case using a beam composed of components of two colors with independent CEP [17]. The study showed a drastic increase

in single particle accelerated energy with the same total laser power. This was due to the pulse beating within the Rayleigh range and the Gouy phase providing an advantageous situation for the particle to slip less out of the region of high accelerating field. Only certain differences in CEP between the different color pulses produced improved kinetic energies, corresponding to the case where the advantageous phase situation is created after the pulses focus, where the acceleration mainly occurs.

This concept of discrete multi-color fields in focus can be generalized to a specific continuous case, where the different colors of a single broadband (ultra-short) driving laser focus to different longitudinal positions. This is known as longitudinal chromatism (LC), which on the collimated beam takes the form of pulse-front curvature (PFC) or a radially varying group delay (for a transform limited pulse). In focus the pulse duration is increased according to the longitudinal separation of the spectral content, resulting in a decreased intensity. This is one of the well known low-order spatio-temporal couplings [18]. LC can be induced simply by focusing via a chromatic singlet lens [19], by using an afocal doublet made of special glasses to apply PFC on the collimated beam to be focused [20], or via a diffractive lens [21] among other methods. We simulate the effect of LC/PFC and chirp on vacuum laser acceleration in the general case, Scenario #1 (related to interaction with a low-density ambient gas) and the restricted case, Scenario #2 (related to interaction with a plasma mirror). As discussed, PFC and LC are equivalent, but to decouple the focusing geometry and the longitudinal chromatism we use the PFC on the collimated beam as the control parameter.

In all of the following simulations we use pulses that have Gaussian spatial and temporal profiles, with $w_0=4\ \mu\text{m}$ and $\tau_0=10\ \text{fs}$ characteristic widths respectively at a central wavelength of 800 nm ($\omega_0=2.35 \times 10^{15}\ \text{rad/s}$). These parameters both fit within the paraxial approximation. Although it has been shown that even in the case of $w_0=4\ \mu\text{m}$ ($5\lambda_0$) the results of acceleration of off-axis particles including non-paraxial terms can be significantly different than the case without, the on-axis case (within $\lambda_0/2$ of the axis) is still valid [22]. Therefore the simulations presented here should be taken as valid only in the on-axis case, and do not provide insight in to acceleration of a beam of electrons with finite extent. Lastly, since the manifestation of the nearfield PFC in focus depends on the focusing geometry, the corresponding near-field width is chosen to be $w_i=4\ \text{cm}$ with a focal length of $f=63\ \text{cm}$.

The longitudinal field of the focused radial polarized field E_z is modeled with near-field PFC α and group delay dispersion (GDD) ϕ_2 in the frequency domain as in [20] using the proper form for the longitudinal field as in [4]. With $A(\omega) = \exp(-\delta\omega^2/\Delta\omega^2)$, $\Delta\omega = 2/\tau_0$, and $\delta\omega = (\omega - \omega_0)$ we have the field around the focus $z = 0$

as

$$\hat{E}_z(z, \omega) = \frac{1}{\Delta\omega} \sqrt{\frac{16P}{\pi\epsilon_0 c}} \frac{A(\omega)}{z_R \left(1 + \left(\frac{z - z_0(\omega)}{z_R}\right)^2\right)} e^{i\phi(z, \omega)} \quad (1)$$

$$\phi(z, \omega) = \Psi_0 + 2 \tan^{-1} \left(\frac{z - z_0(\omega)}{z_R} \right) - \frac{\phi_2 \delta\omega^2}{2} - \frac{\omega z}{c}, \quad (2)$$

with the Rayleigh length $z_R = 2cf^2/\omega_0 w_i^2$, the frequency dependent focus position due to the LC/PFC $z_0(\omega) = 2cf^2\alpha\delta\omega/\omega_0$, the CEP Ψ_0 , and the Fourier-limited pulse power P . In the time domain a positive α corresponds to a positive radial group delay, or the higher frequencies being focused at a higher z . The acceleration of the electron is modeled by the relativistic Lorentz force equations

$$\frac{\partial\beta}{\partial t} = \frac{-q_e E_z(z, t)(1 - \beta^2)^{3/2}}{m_e c} \quad (3)$$

$$\frac{\partial z}{\partial t} = \beta c, \quad (4)$$

with q_e and m_e the elementary charge and electron mass respectively, and $\beta = v/c$. We use a 5th-order Adams-Bashforth finite difference method to have improved accuracy with a fixed step size. Since we only know the field in frequency space, the field $\hat{E}_z(z, \omega)$ must be inverse Fourier transformed to t at each iteration to find the field at the new position $z(t_i)$ and to calculate the next velocity and position. This step significantly increases the computation time compared to the calculations done directly in the time domain (possible only if $\alpha = 0$). The simulations are run until the particle energy is no longer changing significantly, generally in the range of 10 ps for the power levels studied here. Results without any LC/PFC or chirp were compared to those in the literature [4, 15] and agreed very well.

The two specific scenarios are detailed again technically in Fig. 1. In Scenario #1 the simulations start such that the laser pulse is far away from the test particle so as to have no influence, and it propagates across the particle to impart a net kinetic energy. In every simulation — varying laser power, GDD, and LC/PFC — we optimize the initial electron position $z(0)$ and laser CEP Ψ_0 for the maximum final kinetic energy, with the particles always beginning at rest. This emulates an experimental situation where the particles in a low-density gas would be distributed in space and the driving laser would have tunable CEP. In Scenario #2 the simulations start with the laser pulse already at best focus and the electron sitting at the first field zero in front of the field peak, with an initial kinetic energy of 200 keV. This second scenario requires no optimization at each set point

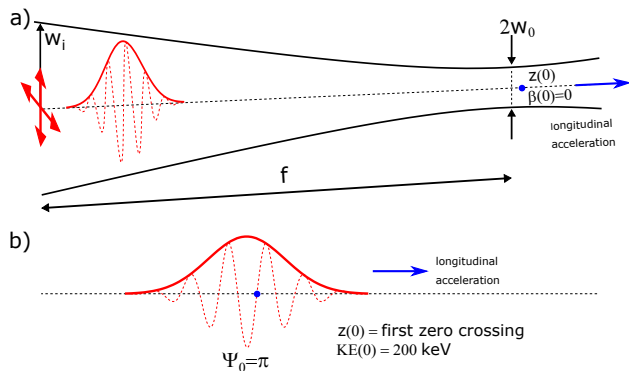


FIG. 1. Sketch of the two scenarios simulated here. These are the more general Scenario #1 (a) and the more restricted Scenario #2 (b). See the text for more details.

due to the restrictions on the electron parameters, but would also require a driving laser with controllable CEP.

For Scenario #1 we find that at pulse energies so as to create few-MeV level electrons (Fourier-limited powers of 80, 90, 100 TW), the addition of LC/PFC has a significant effect on the maximum electron energy after interaction, and the addition of small amounts of chirp can optimize the energy further. This is summarized in Fig. 2. The acceleration decreases for all GDD values when the LC/PFC is zero, matching previous results [23], showing that the effect can only be optimized with non-zero LC/PFC. Note that for the three power levels studied the magnitude of optimum LC/PFC increases, along with the optimum GDD, and also the relative improvement when adding LC/PFC. The optimum LC/PFC is always negative, but the optimum GDD at any amount of LC/PFC always has the same sign as that LC/PFC.

For Scenario #2 we use also laser energies to generate few-MeV level electrons, but in this case it requires significantly less power (Fourier-limited powers of 5, 7, 9 TW) since the electrons have an initial non-zero energy and start immediately at an advantageous phase. Of course, to drive the relativistic plasma-mirror process that this scenario is meant to emulate requires relativistic intensities and therefore higher laser powers. The sub-unity reflectivity of the plasma-mirror and degradation of any other relevant properties would result in a lower effective power taking part in the vacuum laser acceleration after reflection. These complex dynamics are not taken into account, and in fact these simulations only take into account the reflecting laser field, so this must be taken into context when interpreting the results.

The addition of LC/PFC in this scenario also has an effect on the maximum electron energy after interaction, seen in Fig. 3, with the effect and the optimum amount of LC/PFC increasing with the energy of the driving laser as seen before. The effect is however smaller relative to the accelerated energies present, producing only an increase

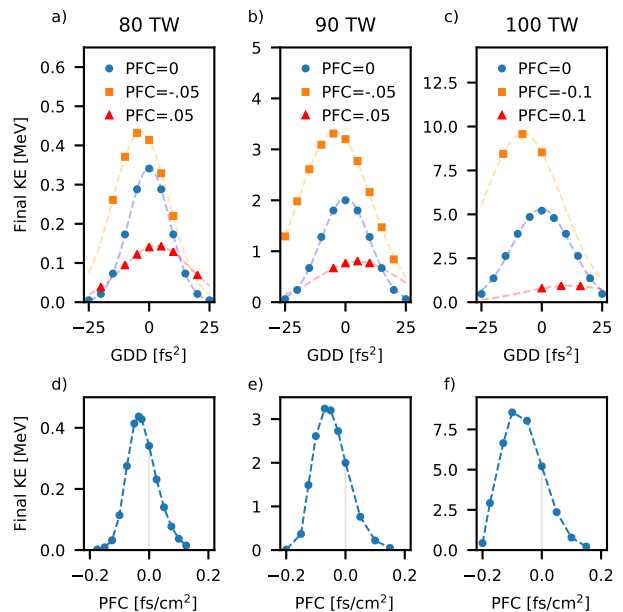


FIG. 2. Results from Scenario #1 with Fourier-limited powers of (a,d) 80, (b,e) 90, and (c,f) 100 TW. The top row (a–c) is final kinetic energies for many combinations of LC/PFC and chirp with the dashed lines Gaussian fits, and the bottom row (d–f) is for zero chirp and various amounts of LC/PFC with the dashed lines as guides for the eyes. LC/PFC is in units of fs/cm^2 always.

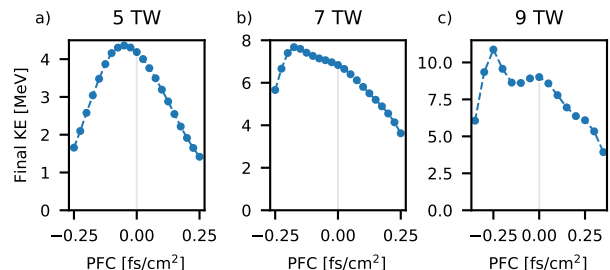


FIG. 3. Results for varying levels of LC/PFC in Scenario #2 with Fourier-limited powers of (a) 5, (b) 7, and (c) 9 TW.

of 21 % in the case of 9 TW driving power. This is due to the fact that the electron begins with non-zero energy, so the advantageous situation does not act as effectively for the parameters resulting in a similar final energy.

The striking result of an increased final kinetic energy with this imparted spatio-temporal coupling (and therefore a slightly lower peak intensity) provides direct motivation for the opportunity to optimize the acceleration process via specific fine-tuning of the LC/PFC. However, this decrease at positive values of LC/PFC provides a useful insight into experiments as well. If there is an undiagnosed level of LC/PFC, then the acceleration process could be either enhanced or damped. For example,

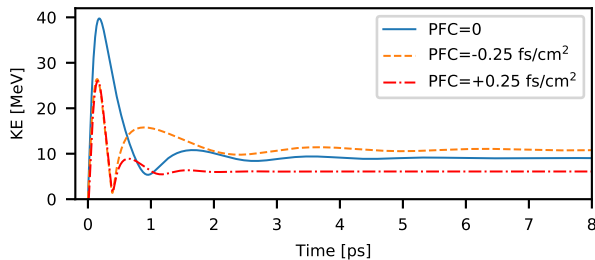


FIG. 4. Comparison of trajectories from Scenario #2 with 9 TW. Shown are the default case (PFC=GDD=0) (solid), the improved case (dashed), and a worsened case (dot-dashed).

in the case of acceleration with a Fourier-limited 90 TW beam a LC/PFC of $+0.05 \text{ fs/cm}^2$ results in a decrease in final kinetic energy by a factor of 2.6 (without any chirp). However, on a beam of $w_i=4 \text{ cm}$ with $f=0.63 \text{ m}$ this level of LC/PFC causes a decrease in peak intensity of only 2.5% and is equivalent to a delay of only 0.8 fs at the edge of the collimated beam. This highlights the sensitivity of the mechanism to LC/PFC. Detailed knowledge of spatio-temporal couplings — possible with developing full spatio-temporal characterization devices [24, 25], or with diagnostics made specifically for measuring PFC [26, 27] — is crucial to not only optimizing the mechanism, but having it perform at a nominal level.

In both scenarios the optimum LC/PFC value is negative, with all positive values of LC/PFC producing lower net acceleration. This corresponds to longer wavelengths being focused to greater z , according to $z_0(\omega)$, meaning that along the acceleration direction the central wavelength is locally increasing within the Rayleigh range. This is a useful way to visualize the effect, analogous to some RF accelerators having increased cavity lengths along the acceleration direction.

In combination with temporal chirp this form of spatio-temporal/spatio-spectral coupling has been explored to control the velocity of the intensity peak of focused laser pulses, a 'Flying Focus' [20, 21], which was the original motivation for this study. However, the magnitudes of LC/PFC and chirp presented are so small such that the velocity of the intensity peak is not significantly affected, rather the effect on the phase within the Rayleigh range is also important. This is required for any effect on vacuum laser acceleration since both LC/PFC and chirp independently reduce the intensity in focus, and for such acceleration the electric field strength and thus intensity are key parameters.

To get a better understanding we can also compare the trajectories of representative simulations, seen in Fig. 4. In both scenarios the optimized case with LC/PFC shows the same general behavior relative to the case without LC/PFC, but for these purposes Scenario #2 is more

straightforward and acts a toy model to view the acceleration only after focus with a constant laser CEP and electron position. With negative LC/PFC the peak energy reached during the peak accelerating half-cycle is lower, but in subsequent laser cycles the electron is decelerated less, and accelerated more, leading to a higher final energy. This is sensible, since the peak field is lower in this main accelerating half-cycle, but the LC/PFC has provided an advantageous situation for the region outside of the intensity peak. This also provides an insight in to why the final kinetic energy is lower with positive LC/PFC. In the case of positive LC/PFC the *peak* kinetic energy is also lower, but the following cycles have a disadvantageous situation and the final kinetic energy is still lower than the default case. This is seen most clearly in comparing the dot-dashed trajectory to the dashed trajectory in Fig. 4 in the time window around 1 ps.

The results in other focusing conditions, with shorter pulse durations, larger driving laser power, or different central frequency are beyond the scope of this work. However, preliminary simulations show that the effect is different at lower pulse durations. Because the effect of LC/PFC on focused intensity is larger as the pulse duration is decreased, the trade-off between improved accelerating phase and decreased intensity is less able to result in an increased final kinetic energy. So it may be that the LC/PFC is only a detrimental property for other driving laser parameters. Scaling with wavelength is discussed in the literature [4], and the effect of spatio-temporal distortions on acceleration with developing THz sources is also of potential interest. At higher laser powers, shorter durations, or tighter focusing, non-paraxial terms and a different temporal or spectral profile would need to be used for satisfactory accuracy, as has been done for specific cases in the past [28].

Experimentally it is possible to compensate for an existing level of LC/PFC [29], but such compensation or tuning mechanisms are not commonplace or simple. Additionally, LC/PFC can come from many sources in ultrafast laser systems, so it is difficult to remove completely from the final high-power beam without taking great care. Therefore, practically, the results of these studies do provide an avenue for optimization, but the more relevant result may be that the amount of LC/PFC necessary to spoil the mechanism is very small.

The results in summary mean that the specifically applied spatio-temporal coupling of longitudinal chromatism (or pulse-front curvature in the near-field) can increase the final kinetic energy of a single electron accelerated on-axis by a focused ultrashort radially-polarized laser beam. This can be increased further with the addition of small amounts of linear chirp. In the general case of Scenario #1, where the initial particle position and the laser CEP are freely varied, this results in almost doubling the energy when accelerated with a 100 TW beam. In the more restricted case of Scenario #2, meant to emu-

late the case of interaction with a relativistic plasma mirror surface, there is also improvement. In both scenarios simulated there is a drastic decrease of the final kinetic energy at values of positive sign, opposite that of the optimum, motivating the characterization of spatio-temporal couplings in any experiment of this kind. Beyond the impact on on-axis vacuum laser acceleration presented here, specific combinations of other low- or high-order spatial-temporal couplings may prove useful in particle manipulation or engineering specific laser-material interaction.

Funding. The work was supported by the fellowship CEA-Eurotalents.2014–2018 (n° PCOFUND-GA-2013-600382) under the Seventh Framework Program (FP7).

Acknowledgement. The author would like to thank Raphaël Lebrun, Antoine Jeandet, and Fabien Quéré for helpful discussions and comments.

* spencer.jolly@cea.fr

- [1] Y. I. Salamin, *Optics Letters* **31**, 2619 (2006).
- [2] C. Varin, M. Piché, and M. A. Porras, *Physical review E* **71**, 026603 (2005).
- [3] Y. I. Salamin, *Optics Letters* **32**, 90 (2007).
- [4] L. J. Wong and F. X. Kärtner, *Optics Express* **18**, 25035 (2010).
- [5] V. Marceau, A. April, and M. Piché, *Optics Letters* **37**, 2442 (2012).
- [6] V. Marceau, C. Varin, T. Brabec, and M. Piché, *Physical Review Letters* **111**, 224801 (2013).
- [7] A. Sell and F. X. Kärtner, *Journal of Physics B: Atomic, Molecular and Optical Physics* **47**, 015601 (2014).
- [8] C. Varin, V. Marceau, P. Hogan-Lamarre, T. Fennel, M. Piché, and T. Brabec, *Journal of Physics B: Atomic, Molecular and Optical Physics* **49**, 024001 (2016).
- [9] L. J. Wong, K.-H. Hong, S. Carbajo, A. Fallahi, P. Piot, M. Soljačić, J. Joannopoulos, F. X. Kärtner, and I. Kaminer, *Scientific Reports* **7**, 11159 (2017).
- [10] S. Payeur, S. Fourmaux, B. E. Schmidt, J. P. MacLean, C. Tchernikov, F. Légaré, M. Piché, and J. C. Kieffer, *Applied Physics Letters* **101**, 041105 (2012).
- [11] S. Carbajo, E. A. Nanni, L. J. Wong, G. Moriena, P. D. Keathley, G. Laurent, R. J. D. Miller, and F. X. Kärtner, *Physical Review Accelerators and Beams* **19**, 021303 (2016).
- [12] P.-L. Fortin, M. Piché, and C. Varin, *Journal of Physics B: Atomic, Molecular and Optical Physics* **43**, 025401 (2010).
- [13] C. Thaury, F. Quéré, J.-P. Geindre, A. Levy, T. Ceccotti, P. Monot, M. Bougeard, F. Réau, P. D’Oliveira, P. Audebert, R. Marjoribanks, and P. Martin, *Nature Physics* **3**, 424 (2007).
- [14] M. Thévenet, A. Leblanc, S. Kahaly, H. Vincenti, A. Vernier, F. Quéré, and J. Faure, *Nature Physics* **12**, 355 (2016).
- [15] N. Zaïm, M. Thévenet, A. Lifschitz, and J. Faure, *Physical Review Letters* **119**, 094801 (2017).
- [16] M. Thévenet, H. Vincenti, and J. Faure, *Physics of Plasmas* **23**, 063119 (2016).
- [17] L. J. Wong and F. X. Kärtner, *Optics Letters* **36**, 957 (2011).
- [18] S. Akturk, X. Gu, P. Bowlan, and R. Trebino, *Journal of Optics* **12**, 093001 (2010).
- [19] Z. Bor, *Optics Letters* **14**, 119 (1989).
- [20] A. Sainte-Marie, O. Gobert, and F. Quéré, *Optica* **4**, 1298 (2017).
- [21] D. H. Froula, D. Turnbull, A. S. Davies, T. J. Kessler, D. Haberberger, J. P. Palastro, S.-W. Bahk, I. A. Begishev, R. Boni, S. Bucht, J. Katz, and J. L. Shaw, *Nature Photonics* (2018), 10.1038/s41566-018-0121-8.
- [22] V. Marceau, C. Varin, and M. Piché, *Optics Letters* **38**, 821 (2013).
- [23] P. Hogan-Lamarre, V. Marceau, C. Varin, T. Brabec, and M. Piché, *2015 European Conference on Lasers and Electro-Optics - European Quantum Electronics Conference*, 2015 European Conference on Lasers and Electro-Optics - European Quantum Electronics Conference , CG_P_19 (2015).
- [24] G. Pariente, V. Gallet, A. Borot, O. Gobert, and F. Quéré, *Nature Photonics* **10**, 547 (2016).
- [25] A. Borot and F. Quéré, *Optics Express* **26**, 26444 (2018).
- [26] Z. Bor, Z. Gogolak, and G. Szabo, *Optics Letters* **14**, 862 (1989).
- [27] Z. Li, N. Miyanaga, and J. Kawanaka, *Optics Letters* **43**, 3156 (2018).
- [28] P. Favier, K. Dupraz, K. Cassou, X. Liu, A. Martens, C. F. Ndiaye, T. Williams, and F. Zomer, *Journal of the Optical Society of America A* **34**, 1351 (2017).
- [29] S.-W. Bahk, J. Bromage, and J. D. Zuegel, *Optics Letters* **39**, 1081 (2014).